Int. J. Heat Mass Transfer. Vol. 31, No. 2, pp. 367–374, 1988
Printed in Great Britain

0017–9310/88 $3.00+0.00

Enhancement of radiative heat transfer in the laminar channel flow of non-gray gases

M. HIRANO,† T. MIYAUCHI and Y. TAKAHIRA
Department of Mechanical Engineering Science, Tokyo Institute of Technology, Ohokayama 2, Meguro, Tokyo 152, Japan

(*Received* 2 *September* 1987)

Abstract—The enhancement of radiative heat transfer based on the multi-band feature of radiative gas is analyzed theoretically for the system of laminar channel flow of high-temperature CO_2 and combustion gases between two parallel heat-absorbing surfaces. An integrodifferential equation of energy conservation, which takes into account the multi-band feature of the radiative gas, is solved numerically, and the enhancement effect by installing a solid plate in the radiative gas is calculated. From the results, it is shown that enhancements of local heat flux of up to 80% for CO_2 and 36% for combustion gas are attainable.

1. INTRODUCTION

ENHANCEMENT of radiative heat transfer is a great theme in developing compact and efficient high-temperature heat exchangers. From this point of view, several studies have been conducted on the enhancement of radiative heat transfer.

Mori *et al.* [1, 2] proposed radiative heat-transfer augmentation by installing a solid plate in the gas flow. The surface of the plate receives heat from the gas by convection and emits radiation to facing heat-absorbing surfaces, thus resulting in the increase of absorbed energy. (Hereafter, we refer to this mechanism as convective–radiative (C–R) conversion.)

Echigo [3] reported an effect of porous medium on radiative heat transfer and proposed another enhancement mechanism based on the radiation shield effect of porous medium.

The authors have proposed a new enhancement mechanism of radiative heat transfer based on the multi-band feature of radiative gas, which is attained by installing a solid plate in the gas [4, 5]. In the previous papers, analysis was conducted for the non-flow system, in which the temperature of the gas was uniform, and the effect of convection neglected. However, in actual heat exchangers, the gas temperature falls gradually as it flows, and not only radiative heat transfer but also convective heat transfer exists. Therefore, it is necessary to analyze this new enhancement mechanism in the flow system in order to apply it to heat exchangers.

In this paper, we conducted an analysis on the laminar channel flow of radiative gases, taking into account their multi-band, non-gray feature, then calculated the increase of the heat-transfer rate and clarified the performance of the newly proposed enhancement mechanism in the flow system. In addition, comparison with the conventional gray analysis was made, and it was clarified that the latter analysis cannot correctly predict this enhancement effect.

2. BASIC EQUATIONS AND SOLUTION METHOD

In order to simulate the radiative heat transfer in high-temperature heat exchangers, we analyzed the system of laminar channel flow of high-temperature gas between two parallel heat-absorbing surfaces. The heat fluxes to the heat-absorbing surfaces were calculated for the cases in which a solid plate is installed or not installed in the midst of flowing gas, and were compared (Fig. 1).

Calculation was done for two gases: CO_2 and a mixture of 8 vol. % CO_2, 16 vol. % H_2O and 76 vol. % N_2, which simulates a typical combustion gas. The gas was assumed to flow into the system with uniform temperature T_e.

In deriving the basic equations, the following assumptions were made.

(1) Both the heat-absorbing surfaces and solid plate surfaces are black.

(2) Temperature of heat-absorbing surfaces is uniform.

(3) As for the heat conduction, we assume that $\lambda(\partial^2 T/\partial x^2) \ll \lambda(\partial^2 T/\partial y^2)$ and that only the heat conduction in the y-direction is taken into account.

(4) As for the gas radiation, we assume that $\partial q_{rx}/\partial x \ll \partial q_{ry}/\partial y$ and that only one-dimensional radiative flux in the y-direction is taken into account.

(5) Flow is fully developed laminar.

(6) The temperature difference between the gas and heat-absorbing surfaces is small, and physical properties are taken as constant.

† MCEC, Mitsubishi Heavy Industries, Ltd., 15–1, Tomihisacho, Shinjuku, Tokyo 162, Japan.

NOMENCLATURE

- A effective bandwidth [m^{-1}]
- A_s slab band absorption [m^{-1}]
- a gray absorption coefficient [m^{-1}]
- c_p specific heat at constant pressure [$J\,kg^{-1}\,K^{-1}$]
- D distance between heat-absorbing surfaces [m]
- E_n exponential integral function for slab gas, $E_n = \int_0^1 \mu^{n-2} \exp(-(t/\mu))\,d\mu$ [dimensionless]
- H distance between heat-absorbing surface and its facing surface [m]
- l thickness of the gas layer [m]
- P pressure [MPa]
- q heat flux [$W\,m^{-2}$]
- R hemispherical total emissive power [$W\,m^{-2}$]
- T temperature [K]
- u flow velocity [$m\,s^{-1}$]
- x coordinate in the flow direction [m]
- y coordinate in the direction perpendicular to the flow [m].

Greek symbols

- γ Euler's constant [dimensionless]
- θ non-dimensional temperature [dimensionless]
- λ thermal conductivity [$W\,m^{-1}\,K^{-1}$]
- μ directional cosine [dimensionless]
- ν wave number [m^{-1}]
- ρ density [$kg\,m^{-3}$]
- σ Stefan–Boltzmann's constant [$W\,m^{-2}\,K^{-4}$]
- τ_H optical depth at band head [dimensionless]
- ω exponential decay width [m^{-1}].

Superscripts and subscripts

- b black body
- c convection
- e value at $x = 0$ (entrance)
- H value at $y = H$ (heat-absorbing surface)
- m bulk mean
- n band number: 1, CO_2 2.7 μm; 2, CO_2 4.3 μm; 3, CO_2 15 μm; 4, H_2O 2.7 μm; 5, H_2O 6.3 μm; 6, H_2O rotation
- r radiation
- s value at solid surface
- w value at heat-absorbing surface
- $'$ with solid plate
- 0 value at $y = 0$.

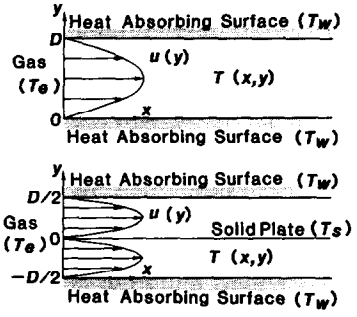

FIG. 1. System analyzed.

To calculate the effective bandwidth and slab band absorption of non-gray gas, the exponential wide-band model proposed by Edwards [6] was used. The model is represented by the following equations:

$$A/\omega = \ln \tau_H + E_1(\tau_H) + \gamma \quad (1)$$

$$A_s(l) = \int_0^{\pi/2} A(l/\cos\Theta) \cdot 2\cos\Theta \sin\Theta\, d\Theta = \int_0^1 A(l/\mu) 2\mu\, d\mu = \omega\{\ln \tau_H + E_1(\tau_H) + \gamma + \tfrac{1}{2} - E_3(\tau_H)\}. \quad (2)$$

As for the radiation (absorption) bands of CO_2, 2.7, 4.3 and 15 μm bands are taken into consideration, while for H_2O, 2.7, 6.3 μm and the rotation bands are taken into account because these bands have major effects on emissivity.

The calculation conditions are chosen as follows:

$$P = 0.1\,\text{MPa}, \quad T_e = 1000°C, \quad T_w = 900°C.$$

For CO_2:

$$D = 0.1\,\text{m}, \quad R_{eD} = \frac{\rho u_m D}{\eta} = 1000, \quad x = 0\text{–}1.0\,\text{m}.$$

For the combustion gas:

$$D = 0.1\text{–}1\,\text{m}, \quad R_{eD} = 1000\text{–}10\,000, \quad x = 0\text{–}1.5\,\text{m}.$$

These values are chosen to meet the typical parameters in the usual high-temperature heat exchangers and to satisfy the assumptions. The physical properties are estimated at 950°C.

The influence of band overlapping, i.e. overlapping of the 2.7 μm bands of CO_2 and H_2O and of the 15 μm band of CO_2 and the rotation band of H_2O, was neglected, but the error caused by this assumption is estimated to be no more than 12% of the emissivity of the gas, according to the result obtained from Hottel's charts [7].

Based on the previous assumptions and conditions, the basic equations and boundary conditions can be given as follows [8].

The velocity profile is

$$u = 6u_m \left\{ \left(\frac{y}{H}\right) - \left(\frac{y}{H}\right)^2 \right\}. \quad (3)$$

The energy conservation equation is

$$\rho c_p u \frac{\partial T}{\partial x} = \lambda \frac{\partial^2 T}{\partial y^2} - \sum_n \left\{ \int_0^y \left. \frac{dA_{sn}(l)}{dl} \right|_{y-y'} \frac{\partial R_b(\nu_n, T(y'))}{\partial T} \frac{\partial T}{\partial y'} dy' - \int_y^H \left. \frac{dA_{sn}(l)}{dl} \right|_{y'-y} \frac{\partial R_b(\nu_n, T(y'))}{\partial T} \frac{\partial T}{\partial y'} dy' \right\} \quad (4)$$

where $H = D$ when the solid plate is not installed, and $H = D/2$ when the solid plate is installed.

Boundary conditions are

$$x \leqslant 0: \quad T = T_e \quad (5)$$

$$x > 0, y = H: \quad T = T_w \quad (6)$$

$x > 0$, $y = 0$: when the solid plate is not installed

$$T = T_w \quad (7)$$

when the solid plate is installed

$$q'_0 = \lambda \left. \frac{\partial T}{\partial y} \right|_0 - \sigma T_s^4 + \sigma T_w^4 - \sum_n R_b(\nu_n, T_w) A_{sn}(H) + \sum_n \int_0^H R_b(\nu_n, T(y')) \left. \frac{dA_{sn}(l)}{dl} \right|_{y'} dy' = 0. \quad (8)$$

The heat flux to the heat-absorbing surface is: when the solid plate is not installed

$$q_H = -\lambda \left. \frac{\partial T}{\partial y} \right|_H - \sigma T_w^4 + \sigma T_w^4 - \sum_n R_b(\nu_n, T_w) A_{sn}(H) + \sum_n \int_0^H R_b(\nu_n, T(y')) \left. \frac{dA_{sn}(l)}{dl} \right|_{H-y'} dy'; \quad (9)$$

when the solid plate is installed

$$q'_H = -\lambda \left. \frac{\partial T}{\partial y} \right|_H - \sigma T_w^4 + \sigma T_s^4 - \sum_n R_b(\nu_n, T_s) A_{sn}(H) + \sum_n \int_0^H R_b(\nu_n, T(y')) \left. \frac{dA_{sn}(l)}{dl} \right|_{H-y'} dy'. \quad (10)$$

The first term on the right-hand side of equations (8)–(10) is a convective term, and the second term is the radiative heat flux from the surface of the plate. The third term is the radiative heat flux from the opposite surface, the fourth term is the absorbed portion of the radiative flux from the opposite surface and the fifth term is the gas radiation through each band.

The energy conservation equation (equation (4)) is a parabolic integrodifferential equation and was solved numerically. In this study, the fully implicit method was used as was done in the previous study [8]. The x derivative was approximated by the forward finite difference, and the second derivative with respect to y was approximated by the central finite difference.

As was reported previously [8], since dA_s/dl of the CO_2 4.3 μm band and the H_2O rotation band has a very steep gradient near $l = 0$ and this results in substantial error in calculating the integral terms, a fine-mesh integration method is adopted near $l = 0$ for these two bands.

The temperature of the solid plate is calculated from equation (8) by using Newton–Raphson's iteration method.

In order to analyze the gray gas case, only the radiation term must be replaced. This was done in accordance with the method reported by Kurosaki [9].

The most adequate gray absorption coefficient must be determined to compare the results with the non-gray ones. As was reported previously [8], we considered the isothermal non-flowing gas of 950°C surrounded by the infinite parallel heat-absorbing surfaces, the temperature of which was 900°C and the distance was D, and determined the gray absorption coefficient which gives the same heat flux to the heat-absorbing surface as the one based on the non-gray analysis.

In the case of CO_2, the gray absorption coefficient a is 0.49 m^{-1} for $D = 0.1$ m. This value was used whether the plate was installed or not.

3. CALCULATED RESULTS

At first, the non-gray analysis was conducted on the previously mentioned condition for CO_2, and the comparison was made between results with and without the solid plate.

Figure 2 shows the distribution of the bulk mean temperature of the gas θ_m along x under the condition of $D = 0.1$ m, $R_{eD} = 1000$, where θ_m is defined by

$$\theta_m = \frac{\int_0^H (T - T_w) u \, dy}{u_m H (T_e - T_w)}. \quad (11)$$

From this figure, it can be seen that the heat transferred to the heat-absorbing surface is increased greatly by installing a solid plate and that the bulk mean temperature decreases remarkably. Also in this figure, the non-dimensionalized solid plate temperature θ_s is shown. It is seen that this temperature is close to that of the heat-absorbing surface.

Figure 3 shows the radiative heat fluxes q_r, q'_r (the summation from the second to the fifth terms on the right-hand side of equations (9) and (10)) and the convective heat fluxes q_c, q'_c (their first term). The prime indicates the value when the solid plate is installed. From this figure, it can be seen that the radiative heat transfer is dominant under this condition. When the solid plate is installed, both radiative and convective heat fluxes are increased but the increase of the former is remarkable. Downstream, both radiative and convective heat fluxes for the case

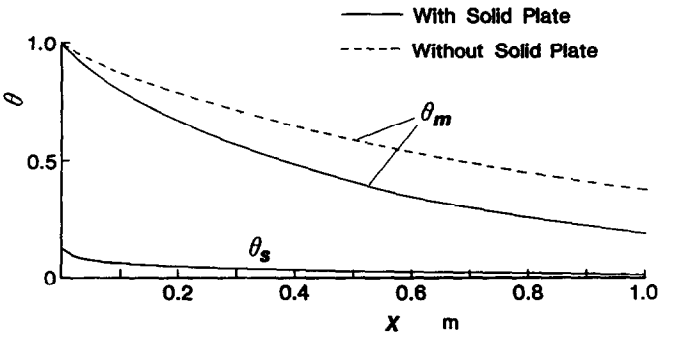

FIG. 2. Distribution of the bulk mean temperature θ_m along x (CO_2 case).

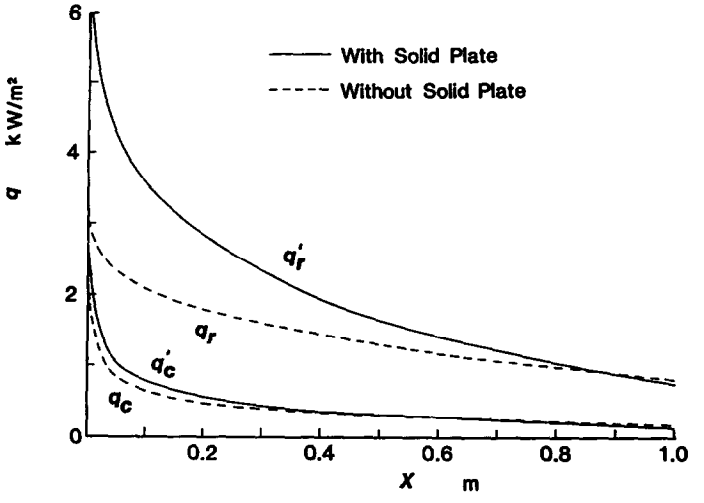

FIG. 3. Distribution of the heat fluxes along x (CO_2 case).

with a solid plate becomes less than those for the case without a solid plate. This is because of the decrease of the gas temperature caused by the heat transfer augmentation.

In order to compare the results on the same basis, the comparison of the total heat flux (the summation of radiative and convective heat fluxes) with and without a solid plate was conducted for the same bulk mean temperature. The result is shown in Fig. 4, in which the ratio q'/q is shown for $1-\theta_m$. From this figure, it can be seen that the total heat flux is increased remarkably by installing a solid plate, and that an augmentation effect of nearly 80% is obtained downstream. In the same figure, the results obtained using the gray gas assumption are shown by a dash-dotted line. The gray analysis predicts the augmentation effect of only 30%, which is far below that obtained by the non-gray analysis.

Figure 5 shows θ_m vs x for the combustion gas, obtained by the non-gray analysis.

The condition is $D = 0.25$ m and $R_{eD} = 2500$. As in the case of CO_2, the bulk mean gas temperature decreased remarkably by installing a solid plate, and the heat-transfer augmentation is obvious.

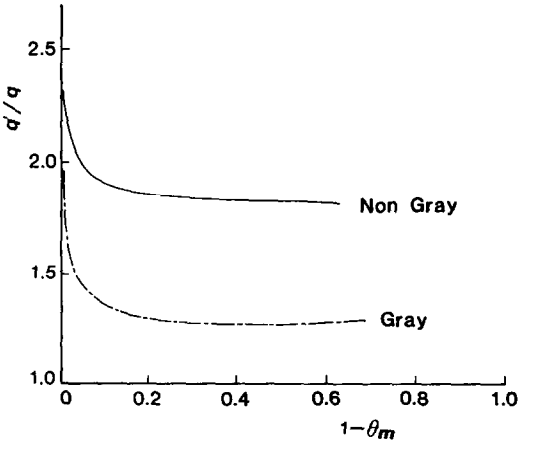

FIG. 4. Augmentation effect (CO_2 case).

From Fig. 6, which shows q_r, q'_r, q_c, q'_c vs x for the combustion gas, it is seen that radiation heat transfer is dominant, and the augmentation effect is mainly due to the increase of radiative heat transfer.

Figure 7, which shows q'/q vs $1-\theta_m$ for the com-

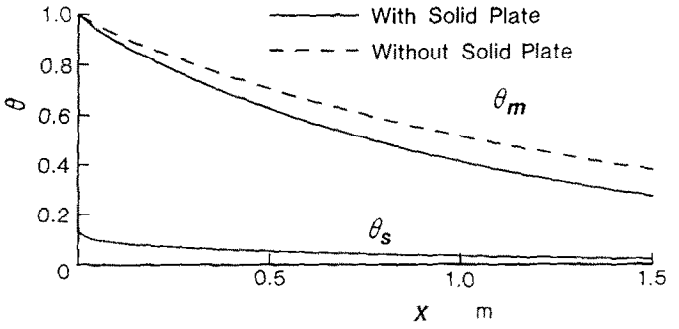

FIG. 5. Distribution of the bulk mean temperature θ_m along x (combustion gas case).

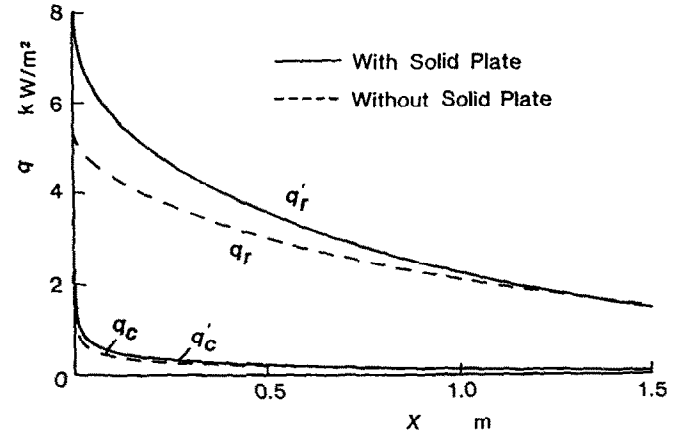

FIG. 6. Distribution of the heat fluxes x (combustion gas case).

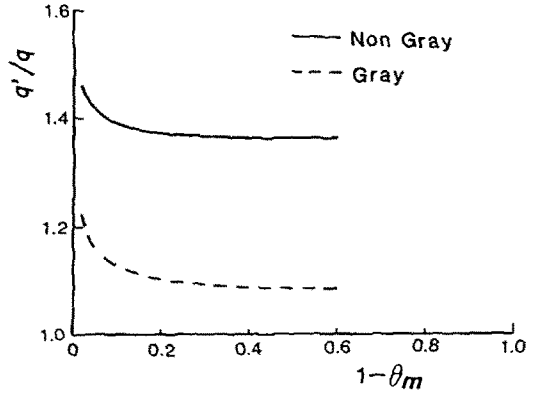

FIG. 7. Augmentation effect (combustion gas case).

bustion gas, indicates that the augmentation effect of nearly 36% is obtained downstream, and that the augmentation effect predicted by the gray analysis is only 8%.

4. DISCUSSION

In the previous papers, we made clear the mechanism of the radiative heat-transfer augmentation in a non-flow system. The essential part of this mechanism is as follows. The solid plate receives radiation from the gas through bands, and emits the same amount of radiative energy because of its adiabatic conditions. Here, the solid plate works as a frequency-converter of radiative energy, i.e. it converts gas band radiation to continuous solid radiation. The absorption of this solid radiation by the gas is small, and most of it reaches the facing heat-absorbing surface. In addition, the heat-absorbing surface directly receives radiation from the gas, and this direct radiation does not significantly decrease as a result of dividing the gas layer by a solid plate, because of the non-linear dependence of gas emissivity on the optical beam length. Therefore, the radiative energy to the heat-absorbing surface with the solid plate exceeds that without the plate.

In the flow system, the surfaces are heated not only by radiation but also by convection, and so the effect of convective heat transfer is added to the above-mentioned mechanism.

Figure 8 shows the relationships between q_{rH}, q_{rw}, q'_{rs}, q_{rg}, q'_{rg}, q_r and q'_r vs $1-\theta_m$. Here, q_{rH} is the radiative heat flux leaving the heat-absorbing surface (the second term on the right-hand side of equations (9) and (10)), q_{rw} and q'_{rs} are the incident radiative heat flux on the heat-absorbing surface from the facing surface (the sum of the third and fourth terms on the right-hand side of equations (9) and (10), respec-

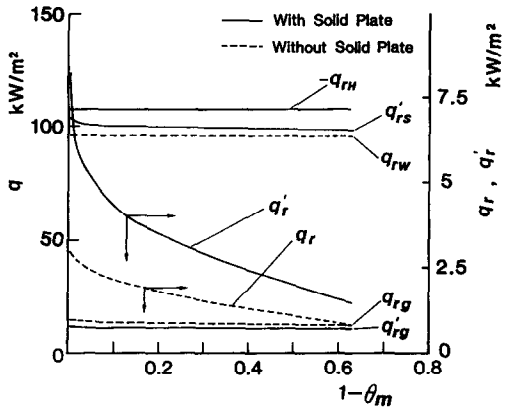

FIG. 8. Details of the radiative heat flux (CO_2 case).

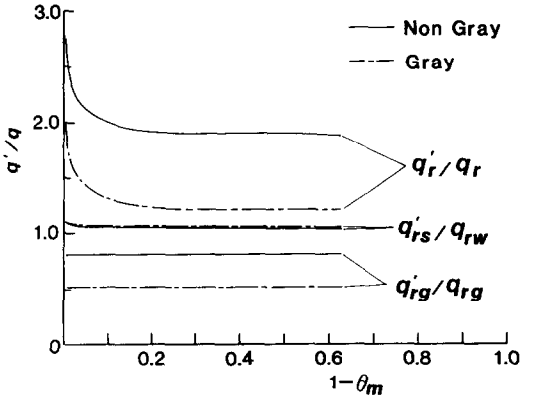

FIG. 9. Comparison with the gray analysis (CO_2 case).

tively), q_{rg} and q'_{rg} are the incident radiative heat flux on the heat-absorbing surface from the gas (the fifth term on the right-hand side of equations (9) and (10), respectively), and q_r and q'_r are the total radiative heat fluxes absorbed by the heat-absorbing surface (the summation of the previous terms). From this figure, it can be seen that the total radiative energy absorbed by the heat-absorbing surface is increased by installing a solid plate in the gas, because the increase of the incident radiative energy to the heat-absorbing surface from the facing surface exceeds the decrease of the incident radiation from the gas.

In the non-flow system, a 50% augmentation effect was obtained for CO_2. In the flow system, however, more than an 80% augmentation effect is obtained. The reason for this is as follows. The solid plate is heated not only by radiative heat transfer but also convective heat transfer, and the temperature of the plate becomes higher and it emits greater radiative energy than in the case of a non-flow system. This additional effect has already been reported by Mori *et al.* [1, 2] as referred to in the introduction.

In Figs. 3 and 6, the convective heat transfer is also increased in the region where $x < 0.4$ m. This is because the width of the channel decreases by half upon installing the plate and the gradient of the flow velocity near the wall becomes steeper; thus, the thermal boundary layer becomes thinner. This effect also contributes to the augmentation.

Incidentally, q'_r is comparatively great in the entrance region. This is because the thickness of the thermal boundary layer is thin and convective heat transfer is high in this region, thus, the temperature of the solid plate becomes higher and emits a large amount of radiative energy to the heat-absorbing surface.

In Figs. 4 and 7, it is shown that the gray analysis predicts a very small augmentation effect compared to that of the non-gray analysis. In order to examine the reason for this, the comparison of q'_{rg}/q_{rg}, q'_{rs}/q_{rw} and q'_r/q_r for non-gray analysis and gray analysis are made in Fig. 9 for the case of CO_2. From this figure, it can be seen that there is no great difference in q'_{rs}/q_{rw} between the non-gray and gray analysis, but that q'_{rg}/q_{rg} differs greatly. The gray analysis predicts an excessive decrease in q_{rg} when the plate is installed, and, hence, it predicts a very small augmentation effect.

This defect of the gray analysis was already pointed out in the previous papers for the non-flow system [4, 5]. By this defect, gray analysis does not predict any augmentation effect in the non-flow system. However, in the flow system, gray analysis predicts a certain amount of augmentation as a result of C–R conversion. In this sense, the result of the gray analysis can be regarded as the 'net' effect of C–R conversion.

Figure 10 shows the relationship between the distance D and q'/q in the downstream region where the enhancement effect becomes nearly constant.

The gray analysis predicts more than 20% of the augmentation effect when D is small ($D < 0.1$ m), but only 5% of this effect when D is large ($D > 0.5$ m). Because the gray analysis indicates the net effect of C–R conversion, these results can easily be explained as follows. The portion of convective heat transfer in the total heat-transfer rate is comparatively large when D is small, but it decreases as D increases.

The non-gray analysis predicts more than 50% of

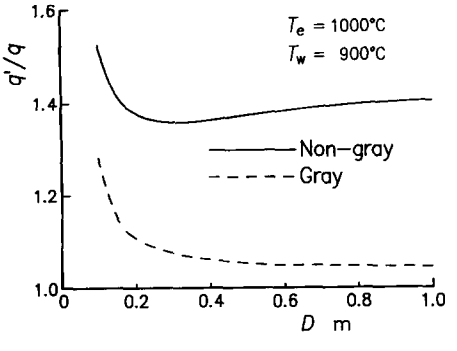

FIG. 10. Dependence of the augmentation effect on distance D (combustion gas case).

the augmentation effect for small D because of the additional C–R augmentation effect. It still predicts a comparatively large value (nearly 40%) for large D. Therefore, it is concluded that the radiative heat-transfer augmentation based on the non-gray feature of radiative gas is dominant when D is large.

5. CONCLUSIONS

In order to investigate the performance of the new enhancement mechanism of radiative heat transfer in the flow system, which is based on the multi-band, non-gray feature of a radiative gas, analysis was conducted for the system of laminar channel flow of high-temperature CO_2 and combustion gas between two parallel heat-absorbing surfaces. The following conclusions were obtained.

(1) By installing a solid plate in the gas, an augmentation effect of nearly 80% for CO_2 and 36% for combustion gas is attained.

(2) These values exceed the ones obtained in the non-flow system [4, 5], due to the additional effect of convective heat transfer.

(3) As the distance between the heat-absorbing surfaces increases, the contribution of the convective heat transfer becomes small, and the augmentation mechanism based on the non-gray feature of radiative gas becomes dominant.

(4) The analysis using the conventional gray gas assumption underestimates the enhancement effect due to the overestimation of the decrease of the radiative heat flux from the gas by dividing the gas layer by the plate.

Acknowledgement—The authors are grateful to Professor Y. Mori, University of Electro-Communications, for his advice on our study. We also thank Professor K. Hijikata, Tokyo Institute of Technology, for his assistance.

REFERENCES

1. Y. Mori, T. Taira and K. Watanabe, Heat exchanger augmentation by radiation plates, ASME Paper No. 76-HT-3, *Proceedings of the ASME–AIChE National Heat Transfer Conference*, St. Louis, Missouri (August 1976).
2. Y. Mori, Performances of heat exchangers on HTGR application, ASME Paper No. 80-HT-39, *Proceedings of the ASME–AIChE National Heat Transfer Conference*, Orlando, Florida (July 1980).
3. R. Echigo, Effective energy conversion method between gas enthalpy and thermal radiation and application to industrial furnaces, *Proceedings of the 7th International Heat Transfer Conference*, Vol. 6, pp. 361–366, Munich (September 1982).
4. M. Hirano, T. Miyauchi and Y. Mori, Enhancement of radiation heat transfer based on multi-bands feature of radiative gases. In *High Temperature Heat Exchangers* (Edited by Y. Mori, A. E. Sheindlin and N. H. Afgan), pp. 172–183. Hemisphere, New York (1986).
5. M. Hirano, T. Miyauchi and Y. Mori, Enhancement of radiative heat transfer based on non-gray feature of radiative gas, *Proceedings of the 8th International Heat Transfer Conference*, Vol. 2, pp. 773–778, San Francisco (August 1986).
6. D. K. Edwards, Molecular gas band radiation. In *Advances in Heat Transfer* (Edited by T. F. Irvine and J. P. Hartnett), Vol. 12, pp. 115–193. Academic Press, New York (1976).
7. W. H. McAdams, *Heat Transmission*, 3rd Edn, pp. 55–125. McGraw-Hill, New York (1954).
8. M. Hirano, T. Miyauchi and Y. Takahira, Heat transfer analysis of non-gray gas in a flow system (1st report, the case of small temperature difference between gas and a heat absorbing surface), *Heat Transfer—Jap. Res.* (1988), in press.
9. Y. Kurosaki, Heat transfer by radiation and other transport mechanism (2nd report, flow between parallel flat plates with simultaneous radiation and convection), *Trans. Japan Soc. Mech. Engrs* **35**(278), 2099–2106 (1969).

AMELIORATION DU TRANSFERT RADIATIF DE CHALEUR DANS UN ECOULEMENT LAMINAIRE EN CANAL DE GAZ NON GRIS

Résumé—L'amélioration du transfert radiatif de chaleur basé sur la représentation multi-bandes d'un gaz est analysée théoriquement pour le cas d'un écoulement laminaire de CO_2 en canal, à haute température et la combustion de gaz entre deux surfaces parallèles absorbantes de chaleur. Une équation intégro-différentielle de conservation d'énergie, prenant en compte le comportement multi-bandes, est résolue numériquement et on calcule l'effet d'amélioration en installant une plaque solide dans le gaz radiatif. A partir des résultats, on montre que les accroissements locaux de flux atteignent jusqu'à 80% pour le CO_2 et 36% pour la combustion de gaz.

VERBESSERUNG DES STRAHLUNGS-WÄRMEAUSTAUSCHES IN EINER LAMINAREN KANALSTRÖMUNG NICHT-GRAU STRAHLENDER GASE

Zusammenfassung—Die Erhöhung des Strahlungs-Wärmeaustausches aufgrund des Strahlungsvermögens in mehreren Band-Bereichen wird für eine laminare Kanalströmung von heißem CO_2 und Verbrennungsgasen zwischen zwei parallelen strahlungsabsorbierenden Platten theoretisch untersucht. Die Integro-Differentialgleichung der Energieerhaltung, welche das Strahlungsvermögen in mehreren Band-Bereichen berücksichtigt, wird numerisch gelöst. Die Erhöhung des Strahlungs-Wärmeaustausches durch den Einbau einer Platte in den Strömungskanal wird berechnet. Die Ergebnisse zeigen, daß eine Erhöhung der örtlichen Wärmestromdichte von bis zu 80% für CO_2 und 36% für Verbrennungsgase erreichbar ist.

ИНТЕНСИФИКАЦИЯ РАДИАЦИОННОГО ТЕПЛОПЕРЕНОСА ПРИ ЛАМИНАРНОМ ТЕЧЕНИИ НЕСЕРЫХ ГАЗОВ В КАНАЛЕ

Аннотация—Теоретически анализируется интенсификация радиационного теплопереноса, обусловленная широкополосным излучением газа при ламинарном течении сильно нагретого CO_2 и выхлопных газов в канале между двумя параллельными теплопоглощающими поверхностями. Численно решено интегро-дифференциальное уравнение сохранения энергии, учитывающее широкополосное излучение газа и рассчитана интенсификация при введении твердотельной пластины в излучающий газ. Результаты показывают, что можно достичь увеличения локального теплового потока до 80% для CO_2 и 36% для выхлопных газов.